Soluble Amyloid β_{1-28}−Copper(I)/Copper(II)/Iron(II) Complexes Are Potent Antioxidants in Cell-Free Systems

Rozena Baruch-Suchodolsky and Bilha Fischer*

Department of Chemistry, Gonda-Goldschmied Medical Research Center, Bar-Ilan University, Ramat-Gan 52900, Israel

Received January 21, 2008; Revised Manuscript Received June 1, 2008

ABSTRACT: Amyloid β (Aβ) is a central characteristic of Alzheimer's disease (AD). Currently, there is a long-standing dispute regarding the role of Aβ−metal ion (Zn, Cu, and Fe) complexes in AD pathogenesis. Here, we aim to decipher the connection between oxidative damage implicated in AD and Aβ−metal ion complexes. For this purpose we study, using ESR, the modulation of Cu/Fe-induced H_2O_2 decomposition by Aβ_{1-28} (Aβ_{28}), a soluble model of A$\beta_{40/42}$. The addition of H_2O_2 to 0.6 nM−360 μM Aβ_{28} solutions containing 100 μM Cu(II)/Cu(I)/Fe(II) at pH 6.6 results in a concentration-dependent sigmoidal decay of [•OH] with IC_{50} values of 61, 59, and 84 μM, respectively. Furthermore, Aβ_{28} reduces 90% of •OH production rate in the Cu(I)−H_2O_2 system in 5 min. Unlike soluble Aβ_{28}, Aβ_{28}−Cu aggregates exhibit poor antioxidant activity. The mode of antioxidant activity of soluble Aβ_{28} is twofold. The primary (rapid) mechanism involves metal chelation, whereas the secondary (slow) mechanism involves •OH scavenging and oxidation of Cu(Fe)-coordinating ligands. On the basis of our findings, we propose that soluble Aβ may play a protective role in the early stages of AD, but not in healthy individuals, where Aβ's concentration is nanomolar. Yet, when Aβ−metal ion complexes undergo aggregation, they significantly lose their protective function and allow oxidative damage to occur.

Highly reactive OH radicals are implicated in many pathological conditions including cancer, diabetes, Parkinson disease, heart diseases, and aging (*1–3*). Harmful OH radicals attack any component in living organisms, including proteins, DNA, and lipids, at the rate of 10^9 to 10^{10} M^{-1} s^{-1} (*4*). These deleterious species are generated from the less damaging reactive oxygen species, superoxide radical anion and hydrogen peroxide (*5*). Fe(II) or Cu(I) ions catalyze H_2O_2 decomposition resulting in OH radical formation (Fenton reaction): Fe(II) + H_2O_2 → Fe(III) + OH• + OH^- (*6–8*).

The decomposition of H_2O_2 to produce •OH is also induced by Cu(II) or Fe(III) ions (Haber−Weiss-like mechanism) (*9–11*), shown here for Cu(II) ion (eqs 1−4) (*12, 13*):

$$Cu(II) + H_2O_2 \rightarrow Cu(I)^{\bullet}O_2H + H^+ \quad (1)$$

$$Cu(I)^{\bullet}O_2H + H_2O_2 \rightarrow Cu(I) + O_2 + {}^{\bullet}OH + H_2O \quad (2)$$

$$Cu(I) + H_2O_2 \rightarrow Cu(II) + {}^{\bullet}OH + OH^- \quad (3)$$

$$3H_2O_2 \rightarrow O_2 + 2{}^{\bullet}OH + 2H_2O \quad (4)$$

Hydrogen peroxide and deleterious OH radicals were proposed to trigger neurotoxicity also in Alzheimer's disease (AD) (*14–16*).

AD brain tissue is characterized by amyloid plaques, the major component of which is amyloid β (Aβ) peptide, a 39−43 amino acid residue peptide (*17, 18*). Amyloid deposition is probably a critical step in the neurodegenerative process associated with AD (*19*). In addition, AD brain tissue is characterized by unusually high concentrations of zinc, copper, and iron ions (*20*).

Thus, Cu(II) and Fe(III) have been found in abnormally high concentrations in amyloid plaques (~0.4 and 1 mM, respectively) (*21*). Furthermore, Aβ in vitro (and in vivo) binds these metal ions with high affinity (*22, 23*). Raman microscopy studies identified both Cu and Zn bound to histidine residues in amyloid core plaques (*24*). A recent study proposed that the Cu(II) ligands of Aβ_{28}, a model of natural Aβ, are Asp1 and His6, His13, and His14 (*23*).

Excessive Cu(II) binding, and to a lesser extent Fe(III) binding (*25*), of Aβ may have a deleterious effect on promoting the aggregation and the redox activities of the Aβ proteins (*26*). Aβ has been shown to be toxic in vitro (*27–30*). High concentrations of Aβ incubated with Cu(II) were neurotoxic to primary neurons (*31, 32*). Likewise, Aβ dissolved in Fe(III)-containing media was toxic to neurons (*33, 34*). Several studies showed that the structural transition (from random coil to β-sheet) from monomeric to fibrillar peptide was required for toxicity (*35, 36*). Other studies indicated that the presence of transition metals may be required for both Aβ fibrillization and the initiation of reactive oxygen species (ROS) generation. Thus, the reduction of metal ions by Aβ (*31, 37*) and of A$\beta_{40/42}$ by other cellular reductants allows Aβ to produce H_2O_2 from O_2 and, hence, act as an *oxidant*, as shown for cell cultures in the presence of Cu(II) (*33, 37, 38*).

Specifically, A$\beta_{40/42}$ N-terminal 14 residues, coordinate Cu(II) or Fe(III) ions (*39*). Reduction of Cu(II) (or Fe(III) (*37*)) ions, in A$\beta_{40/42}$ complex, to Cu(I) results in H_2O_2 in vitro formation from molecular oxygen (*31*). The simultaneous production of Cu(I) and H_2O_2 by Aβ raises the

* Author to whom correspondence should be addressed. Tel: 972-3-5318303. Fax: 972-3-635-4907. E-mail: bfischer@mail.biu.ac.il.

10.1021/bi800114g CCC: $40.75
Published on Web 07/04/2008

possibility that OH radical is being formed by Fenton chemistry in AD brains (*31*).

On the other hand, a significant amount of evidence indicates the contrary, that the formation of diffuse amyloid plaques may be considered as a compensatory response that reduces oxidative stress (*40, 41*) and that the accumulation of Aβ in the AD brain may be related to the increased oxidative challenge experienced by the brain as we age (*42*).

Evidence pointing at either an *antioxidant* or *oxidant* function of $A\beta_{40/42}$ was thoroughly reviewed by Atwood et al. (*43*).

It was suggested that the strong chelating properties of Aβ for Cu(II) and Zn(II) (and perhaps Fe(III)) indicate that one of Aβ functions is the sequestration of these metal ions and the removal of these potentially redox-active species from oxidative reactions. Various studies have demonstrated that $A\beta_{40/42}$ exhibits neuroprotective properties when present at physiological concentrations (nanomolar) (*44*). This antioxidant activity is observed both intra- and extracellularly in diffuse amyloid deposits, CSF, and plasma. Evidence that Aβ has *antioxidant* activity is accumulating (*45–49*).

Atwood et al. proposed the following solution to the apparent contradiction concerning the oxidant/antioxidant function of Aβ (*43*): Increased generation of Aβ following oxidative stress indicates a response to preserve normal cellular function by reducing oxidative insults. However, at some threshold level of ROS generation, efficient removal of Aβ−metal complexes would be overtaken by their disproportionably high generation, resulting in the uncontrollable growth of plaques. This growth consequently may overwhelm antioxidant defense systems incapable of handling the accumulating H_2O_2. Thus, Aβ−Cu deposits are predicted to be neurotoxic if H_2O_2 is produced above the threshold level of removal. This results in a vicious cycle of increased Aβ generation and ROS production leading to neurotoxicity (*50*).

Therefore, to accelerate oxidation, Aβ must be present in concentrations that greatly exceed those normally measured in biological fluids or tissues (i.e., micromolar vs nanomolar) (*51, 52*). This finding has been reported for cerebrospinal fluid, where Aβ acts as an *antioxidant* at 0.1−1.0 nM concentrations, while at higher Aβ concentrations its antioxidant action is abolished (*49*).

The apparent confusion regarding the antioxidant/prooxidant properties of $A\beta_{40/42}$ emphasizes the urgent need to systematically explore the modulatory role of $A\beta_{40/42}$ at oxidative stress conditions. For this purpose, we decided to study the modulation of ·OH generation by Aβ under oxidative conditions in a cell-free system. In this way we expected to gain fundamental knowledge on pathophysiological mechanisms of AD at the molecular level.

To *directly* explore the modulation of OH radical production from H_2O_2 *by A*β, we targeted removing the immense complexity and numerous cross-interactions occurring in cells and focusing on the "naked" Aβ in the simplest oxidative system possible, namely, Cu(I)/Cu(II)/Fe(II) in the presence of H_2O_2. Furthermore, we selected $A\beta_{1-28}$ ($A\beta_{28}$) as a soluble model of $A\beta_{40/42}$.

$A\beta_{28}$ is a common soluble model for studies of $A\beta_{40/42}$ function (*23, 26, 53, 54*), which can also serve as a model for aggregated $A\beta_{40/42}$ (*55*). However, unlike $A\beta_{40/42}$, $A\beta_{28}$ is incapable of reducing Cu(II) and Fe(III). Therefore, in our studies we used Cu and Fe ions in their highly reactive, low valence form (i.e., Cu(I) and Fe(II)), in addition to Cu(II) ions.

Furthermore, as most data on Aβ refer only to its catalytic activity to dismutate $O^{2-\bullet}$ to H_2O_2, we intended to study here the effect of Aβ on the metal-induced H_2O_2 decomposition to OH radicals.

In addition, we wanted to test the hypothesis that high concentrations of Aβ (i.e., micromolar vs nanomolar) are toxic (*51, 52*) and that toxicity depends on the metal ion type (i.e., Cu vs Fe). Moreover, we wanted to learn if aggregation changes the modulatory function of soluble $A\beta_{28}$.

For these purposes, we studied by ESR[1] $A\beta_{28}$ in the above simplified oxidative systems using 5,5′-dimethyl-1-pyrroline *N*-oxide (DMPO) as a spin trap. Specifically, we explored the effect of the following parameters on Aβ's modulation of metal ion induced H_2O_2 decomposition: Aβ's concentration, Aβ's solubility, metal ion type, and time.

EXPERIMENTAL PROCEDURES

Materials. $FeSO_4 \cdot 7H_2O$ was purchased from J. T. Baker Inc. (Phillipsburg, NJ). Copper nitrate (10 g/L) standard solution was purchased from Merck. Tetrakis(acetonitrile)-copper(I) hexafluorophosphate and bicinchoninic acid disodium salt (BCA) were purchased from Aldrich Chemical Co. Thioflavin-T, Congo red, DMPO, and amyloid β−protein fragment 1−28, were purchased from Sigma Chemical Co. Hydrogen peroxide (30% solution) was obtained from Frutarom Ltd. (Haifa, Israel). $Cu(CH_3CN)_4PF_6$ was purified before use by dissolving the salt in acetonitrile (HPLC grade) and filtering the undissolved Cu(II) salt by a syringe nylon 0.45 μm filter. The filtrate was deaerated with argon stream. $FeSO_4 \cdot 7H_2O$ was recrystallized twice from water−ethanol before use. The concentration of the Cu(I) salt was determined by UV spectroscopy by the addition of the specific Cu(I) indicator, BCA ($\epsilon_{562nm} = 7700\ M^{-1}$) (*56*). As a negative control we have performed the following measurement: $A\beta_{28}$−Cu(II) solution was prepared by adding 1 mM $Cu(NO_3)_2$ in HPLC grade water (50 μL) to 0.6 mM $A\beta_{28}$ solution (50 μL), after mixing for 30 s. BCA (0.14 M, 3 μL) was added and HPLC grade water up to 2 mL (total volume). This solution was analyzed during 24 h by UV measurements. No signal was observed at 562 nm (indicative of the presence of only Cu(I)).

Aqueous solutions were freshly prepared with HPLC grade water (BioLab Ltd., Israel). The spin trap DMPO was purified by mixing a spatula of activated charcoal with 1 mL of ca. 0.4 M DMPO solution for about 30 min in the dark. The solution was then filtered, and the exact concentration of DMPO was determined by UV spectroscopy ($\epsilon_{228nm} = 8000\ M^{-1}$) (*57*). DMPO solution was deaereted with an argon stream and stored at −18 °C for no longer than 2 weeks after purification. All other commercial products were used without any purification. Crude $A\beta_{28}$ was purified by HPLC over a Chromolith performance RP-18E column, 100 × 4.6 mm, applying a linear gradient of 13% to 45% B in 30 min (A is 0.1% TFA in H_2O and B is 3:1 acetonitrile:A). The

[1] Abbreviations: ESR, electron spin resonance; DMPO, 5,5′-dimethyl-1-pyrroline *N*-oxide; Tris, tris(hydroxymethyl)aminoethane; BCA, bicinchoninic acid disodium salt.

solution of the purified peptide was filtered over a PVDF 0.45 μm filter. The peptide purity was determined by ^{1}H NMR using a pure reference. The pure freeze-dried Aβ_{28} was dissolved in water (HPLC grade) to give 0.6−1.2 mM stock solutions; the stock solutions were stored at −20 °C. Due to the limited solubility of Aβ_{28} it was impossible to obtain more concentrated solutions. The concentration of soluble Aβ_{28} was based on UV measurements using the extinction coefficient of tyrosine residue (ϵ 1280 at 280 nm) (*58*). UV data were consistent with amino acid analysis.

General. OH radicals produced from H_2O_2 by Fe(II) or Cu(I/II) ion catalysis were detected by ESR spectroscopy using a Bruker ER 100d X-band spectrophotometer. ESR settings were as follows: microwave frequency, 9.76 GHz; modulation frequency, 100 kHz; microwave power, 6.35 mW; modulation amplitude, 1.2 G; time constant, 655.36 ms; sweep time, 83.89 s; and receiver gain, 2×10 (*5*) for Fe(II)−H_2O_2 and Cu(I)−H_2O_2 systems or 2×10^6 for Cu(II)−H_2O_2 system. After acquisition, the spectra were processed by the Bruker WIN-EPR software version 2.11 for integrating the signals. The integration of the second signal of the DMPO−OH spin adduct quartet is expressed as a percentage of the control (control solutions contained only Cu(I/II) or Fe(II)−H_2O_2 solutions). ESR measurements were repeated 2−5 times on different days. Absorption data were measured on a Shimadzu UV−vis recording spectrophotometer, UV-2401PC.

OH Radical Production Assay. Two millimolar Cu($CH_3CN)_4PF_6$ in acetonitrile (5 μL) or 1 mM Cu($NO_3)_2$ (10 μL) or 1 mM $FeSO_4$ (10 μL) was added to 0.06−1.4 mM Aβ_{28} stock aqueous solutions (1−30 μL). After an incubation period of 30 s, 1 mM Tris buffer, pH 7.4, (40−75 μL) was added to Aβ_{28}−Cu/Fe ion solutions. After mixing for 2 s, 20 mM DMPO (10 μL) was quickly added followed by 0.1 M H_2O_2 (10 μL). Final component concentrations in 100 μL total volume: 0.1 mM $FeSO_4$/Cu($NO_3)_2$/Cu($CH_3CN)_4PF_6$, 0.6 nM−0.36 mM Aβ_{28}, 2 mM DMPO, and 10 mM H_2O_2. Final pH values of the Fe(II), Cu(I), and Cu(II) systems were 6.61 ± 0.01, 6.62 ± 0.01, and 6.60 ± 0.01, respectively. ESR measurement was performed 150 s (for Cu(I) and Fe(II)) and 20 min (for Cu(II)) after the addition of H_2O_2. All final solutions of Cu($CH_3CN)_4PF_6$ contained 5% v/v acetonitrile.

Monitoring the Kinetics of Aβ_{28}-Modulated Cu/Fe H_2O_2 Decomposition. (A) Control samples were prepared by adding 1 mM $FeSO_4$ (10 μL) or 1 mM Cu($NO_3)_2$ (10 μL), or 2 mM Cu($CH_3CN)_4PF_6$ in acetonitrile (5 μL) to 1 mM Tris buffer (70, 70, and 75 μL, respectively, pH 7.4). After mixing for 2 s, 20 mM DMPO (10 μL) was added quickly followed by 0.1 M H_2O_2 (10 μL). Final component concentrations in 100 μL total volume: 0.1 mM $FeSO_4$/Cu($CH_3CN)_4PF_6$, 2 mM DMPO, and 10 mM H_2O_2. (B) Soluble amyloid β samples were prepared by adding 2 mM Cu($CH_3CN)_4PF_6$ in acetonitrile (5 μL) or 1 mM Cu($NO_3)_2$ (10 μL) or 1 mM $FeSO_4$ (10 μL) to 0.6−1.4 mM Aβ_{28} stock solutions (1−30 μL). After an incubation period of 30 s, 1 mM Tris buffer, pH 7.4 (40−75 μL), was added to Aβ−Cu/Fe complex solutions. After mixing for 2 s, 20 mM DMPO (10 μL) was quickly added followed by the addition of 0.1 M H_2O_2 (10 μL). Final component concentrations in 100 μL total volume: 0.1 mM $FeSO_4$/Cu($NO_3)_2$/Cu($CH_3CN)_4PF_6$, 0.024−0.36 mM Aβ_{28}, 2 mM DMPO, and 10 mM H_2O_2. (C) Aggregated Aβ_{28}−Cu(I) sample was prepared by adding 11 mM Cu($CH_3CN)_4PF_6$ in acetonitrile (1 μL) to 0.6 mM Aβ_{28} solutions (10 μL); after short mixing, the pH was adjusted to 7.4 (0.025 M NaOH (2 μL)). The sample was incubated at room temperature for 30 min to allow the aggregates to mature. Then, 1 mM Tris buffer, pH 7.4 (67 μL), was added to Aβ_{28}−Cu(I) complex solution. After mixing for 2 s, 20 mM DMPO (10 μL) was quickly added followed by the addition of 0.1 M H_2O_2 (10 μL). Final component concentrations in 100 μL total volume: 0.1 mM Cu($CH_3CN)_4PF_6$, 0.06 mM Aβ_{28}, 2 mM DMPO, and 10 mM H_2O_2. Samples were scanned in 2−5 min time intervals. Kinetic data are presented as the amount of DMPO−OH adduct, represented by integration of the second peak of the DMPO−OH adduct quartet, vs time.

Characterization of Aβ_{28}−Cu(I) Aggregates. Aβ_{28}−Cu(I) aggregates were prepared by adding 11 mM Cu($CH_3CN)_4PF_6$ in acetonitrile (1 μL) to 0.6 mM Aβ_{28} solution (10 μL); after mixing for 10 s, the pH was adjusted to about 7.5 by NaOH (0.025 M NaOH (4 μL)). Final component concentrations: 0.2 mM Cu($CH_3CN)_4PF_6$ and 0.12 mM Aβ_{28}. The sample was matured for 2 days at room temperature to obtain aggregates. **(A)** *TEM sample* was prepared by applying 3 drops of Aβ_{28}−Cu(I) aggregate suspension (see preparation above) on a grid; water was vaporized, by allowing the grid to stand at room temperature overnight. **(B)** *ICP sample* was prepared by adding 11 mM Cu($CH_3CN)_4PF_6$ in acetonitrile (10 μL) to 0.6 mM Aβ_{28} aqueous solutions (100 μL); after mixing for 10 s, the pH was adjusted to about 7.5 by NaOH (0.025 M NaOH (20 μL)). Final concentration of components: 0.1 mM Cu($CH_3CN)_4PF_6$ and 0.06 mM Aβ_{28}. The sample was left overnight at room temperature to obtain mature aggregates. Then the aggregates were diluted with HPLC grade water to a final volume of 1 mL, followed by filtration of the aggregates over a 13 mm 0.45 μm nylon Restek syringe filter, taking advantage of the protein-absorbing property of this filter (proved by the disappearance of Aβ_{28}'s peak upon HPLC analysis of the filtrate). The filtrate was diluted to a final volume of 5 mL and assayed by ICP. The filtrate contained 0.79 μM free Cu out of the original 0.1 mM Cu in the ESR Aβ_{28}−Cu(I) ESR sample. **(C)** *ICP control experiment:* 0.025 M NaOH (20 μL) was added to 11 mM Cu($CH_3CN)_4PF_6$ in acetonitrile (1 μL) and incubated overnight. This solution was diluted to 1 mL with HPLC grade water. The sample was filtered over a 13 mm 0.45 μm nylon Restek syringe filter. The filtrate was diluted to 5 mL with HPLC grade water, and the sample was subjected to ICP measurement. The Cu concentration found by ICP was 0.14 ± 0.04 mg/L, and the calculated concentration was 0.1398 mg/L.

(D) *Thioflavin-T (ThT) Assay (59, 60).* A control sample, containing ThT and Cu(I), was prepared by adding 10 mM Cu($CH_3CN)_4PF_6$ in acetonitrile (6 μL) to ThT (3 mL, 50 μM in PBS buffer, pH 7.4). The actual sample contained ThT (3 mL, 50 μM in PBS buffer, pH 7.4) and Aβ fibril solution (fibrils were prepared by mixing 0.6 mM Aβ solutions (60 μL), 10 mM Cu($CH_3CN)_4PF_6$ in acetonitrile (6 μL), and 0.025 M NaOH solutions (12 μL) as described above). Final component concentrations in a 3 mL sample: 50 μM ThT, 20 μM Cu(I), and 12 μM Aβ fibrils. The typical Aβ fibril-bound dye emits at 482 nm (excitation at 450 nm). **(E)** *Congo Red Assay (59, 61).* Two millimolar Congo red stock solution was prepared in PBS (pH 7.4) and filtered

three times on a cotton-plugged Pasteur pipet. Control sample, containing Congo red and Cu(I), was prepared by adding 10 mM $Cu(CH_3CN)_4PF_6$ in acetonitrile (2 μL) to 5 μL of Congo red stock solution; PBS buffer was added to a final sample volume of 1 mL. The actual sample contained 5 μL of Congo red stock solution and $A\beta_{28}$ fibril solutions (fibrils were prepared by mixing 0.6 mM $A\beta_{28}$ stock solution (20 μL), 10 mM $Cu(CH_3CN)_4PF_6$ in acetonitrile (2 μL, and 0.025 M NaOH solution (4 μL) as described above); PBS buffer was added to a final sample volume of 1 mL. Final component concentrations in 1 mL sample: 10 μM Congo red, 20 μM Cu(I), and 12 μM $A\beta_{28}$ fibrils. The typical $A\beta$ fibril-bound dye absorbs at 490 nm.

Analysis of $A\beta_{28}$ Peptide Composition under Oxidative Conditions. Samples were prepared by adding 2 mM $Cu(CH_3CN)_4PF_6$ in acetonitrile (5 μL) or 1 mM $Cu(NO_3)_2$ (10 μL) or 1 mM $FeSO_4$ (10 μL) to 0.6 mM $A\beta_{28}$ solution (10 μL). After an incubation period of 30 s, 1 mM NH_4HCO_3 buffer, pH 7.4 (75 or 70 or 70 μL, respectively), was added to $A\beta_{28}$−Cu/Fe complex solutions. After mixing for 2 s, 0.1 M H_2O_2 (10 μL) was quickly added. Final component concentrations in 100 μL total volume: 0.1 mM $Cu(CH_3CN)_4PF_6$ or $Cu(NO_3)_2$ or $FeSO_4$, 0.06 mM $A\beta_{28}$, and 10 mM H_2O_2. Control sample contains 0.1 mM $Cu(CH_3CN)_4PF_6$ or $Cu(NO_3)_2$ or $FeSO_4$, 0.06 mM $A\beta_{28}$, without H_2O_2. Altogether there were 13 samples: (1) 0.06 mM $A\beta_{28}$; (2) 0.06 mM $A\beta_{28}$, 0.1 mM $Cu(CH_3CN)_4PF_6$ incubated for 4 min (control); (3) 0.06 mM $A\beta_{28}$, 0.1 mM $Cu(CH_3CN)_4PF_6$, and 10 mM H_2O_2 incubated for 4 min; (4) 0.06 mM $A\beta_{28}$, 0.1 mM $Cu(CH_3CN)_4PF_6$ incubated for 24 h (control); (5) 0.06 mM $A\beta_{28}$, 0.1 mM $Cu(CH_3CN)_4PF_6$, and 10 mM H_2O_2 incubated for 24 h; (6) 0.06 mM $A\beta_{28}$, 0.1 mM $FeSO_4$ incubated for 4 min (control); (7) 0.06 mM $A\beta_{28}$, 0.1 mM $FeSO_4$, and 10 mM H_2O_2 incubated for 4 min; (8) 0.06 mM $A\beta_{28}$, 0.1 mM $FeSO_4$ incubated for 24 h (control); (9) 0.06 mM $A\beta_{28}$, 0.1 mM $FeSO_4$, and 10 mM H_2O_2 incubated for 24 h; (10) 0.06 mM $A\beta_{28}$, 0.1 mM $Cu(NO_3)_2$ incubated for 21.5 min (control); (11) 0.06 mM $A\beta_{28}$, 0.1 mM $Cu(NO_3)_2$, and 10 mM H_2O_2 incubated for 21.5 min; (12) 0.06 mM $A\beta_{28}$, 0.1 mM $Cu(NO_3)_2$ incubated for 24 h (control); (13) 0.06 mM $A\beta_{28}$, 0.1 mM $Cu(NO_3)_2$, and 10 mM H_2O_2 incubated for 24 h. *Amino Acid Analysis*. Amino acid quantity was calibrated vs hydrolysis stable amino acids (Arg, Ala, Val). The "calibration factor" represents quantity, in picomoles, of one hydrolytically stable amino acid. Therefore, the "calibration factor" equals 100%. $A\beta_{28}$ contains 1 Arg, 2 Ala, and 3 Val. The "calibration factor" is an average of these three amino acids in picomole units: $[Arg_{(pmol)} + (Ala_{(pmol)}/2) + (Val_{(pmol)}/3)]/3$. Oxidative damage to $A\beta_{28}$ was measured by calculating the quantity of the His residues in $A\beta_{28}$. $A\beta_{28}$ contains 3 His; therefore, the quantity of His in the peptide was calculated by $100(His_{(pmol)}/3)$/ "calibration factor".

RESULTS AND DISCUSSION

Establishing ESR Experimental Conditions. **(A)** *Validity of $A\beta_{28}$ Model*. Studying metal binding by the endogenous $A\beta_{40/42}$ is plagued by many difficulties, particularly aggregation of the peptides (*62*).

Owing to the propensity of $A\beta_{40/42}$ to aggregate, shorter peptides containing the Cu-binding portion are often studied as models for a soluble Cu−$A\beta_{40/42}$ complex. Such soluble model complexes are of relevance, because it is thought that soluble complexes of Cu−$A\beta_{40}$ are formed prior to aggregation. $A\beta_{28}$ can aggregate to fibrils like $A\beta_{40/42}$ at higher concentrations with long incubations (*23*).

We selected $A\beta_{28}$ fragment as a soluble and valid model of $A\beta_{40}/_{42}$, as $A\beta_{28}$ includes both the $A\beta_{40/42}$ hydrophilic N-terminus (residues 1−14) involved in metal ion binding (Asp1, His6, His13, and His14) (*23*) and the central hydrophobic core (residues 15−21 and 24−28) involved in $A\beta$ aggregation (*39*). Indeed, $A\beta_{28}$ produces insoluble β-pleated sheet structures in vitro, similar to the β-pleated sheet structures in amyloid deposits in vivo (*55*). **(B)** *Selection of Redox-Active Metal Ions*. $A\beta_{42}$ was reported to highly stabilize the Cu(I) oxidation state as shown by the extraordinarily high positive potential of $A\beta$−Cu complex (ca. +550−500 mV vs Ag/AgCl electrode, while naked Cu(II) in PBS showed a Cu(II/I) reduction peak at ∼−80 mV) (*31*). A recent report suggested that the redox potential of $A\beta_{42}$−Cu complex was +80 mV vs Ag/AgCl electrode (*63*). Met35 was considered to be critical for the reduction of $A\beta_{40/42}$−Cu(II) and production of $A\beta_{40/42}$−Cu(I) complex (*31, 64*). Yet, recent evidence provided by several groups claimed that Met35 is not involved in Cu(II) reduction but rather cellular reductants (*63, 65, 66*).

In our cell-free experiments, no reducing agents were present. Therefore, to simulate the reactive metal ions at $A\beta_{40/42}$, suspected in inducing OH radical formation (*37*), we studied here Cu(I)− and Fe(II)−$A\beta_{28}$ complexes. In addition to Cu(I) and Fe(II) ions, we studied Cu(II), which also induces H_2O_2 decomposition and OH radical production [eqs 1−4] (*12*). Bush et al. found that Fe(III) is also reduced by $A\beta_{42/40}$ (*37*), however to a significantly lesser amount than Cu(II) reduction under the same conditions (*31*). Therefore, we have not studied Fe(III) ions here. **(C)** *Selection of ESR Measurement Conditions*. ESR was our method of choice for monitoring the effect of $A\beta_{28}$ on the production of $^{\bullet}$OH from Cu/Fe-induced H_2O_2 decomposition. For this purpose, we applied DMPO as a spin trap. The compatibility of DMPO for monitoring radical formation due to Cu(II)-induced hydroperoxide decomposition has been previously demonstrated (*67, 68*). **(D)** *Metal Ion Concentration*. Free Cu(II) ions do not exist in the cytosol (*69*). In amyloid, Cu concentration was measured at ∼0.5 mM (*21*). Therefore, in our studies we used Cu(I/II) concentrations of the same order of magnitude (0.1 mM). For comparison, we studied the Fe(II)−H_2O_2 system also at 0.1 mM Fe(II). **(E)** *$A\beta$ Concentration*. Previously, it was claimed that, to accelerate oxidation, $A\beta$ must be present in concentrations greatly exceeding those normally measured in biological fluids or tissues (i.e., micromolar vs nanomolar) (*51, 52*). To test this hypothesis, we studied $A\beta$ at nanomolar to micromolar concentrations (1 nM−600 μM). **(F)** *Buffer and pH*. ESR samples were prepared in 1 mM Tris buffer, pH 7.4. This was our buffer of choice as it had an excellent buffer capacity even at high $A\beta$ concentrations. At 1 mM Tris concentration, there was a minimal scavenging effect of the buffer (*70*). pH values of Cu(I)− or Cu(II)−H_2O_2 systems were 6.62 ± 0.01 and 6.60 ± 0.01, respectively. No cuprous oxide was obtained at pH 6.62 due to the presence of acetonitrile as a stabilizing ligand (5% v/v). We studied the production of OH radicals relative (as % of control) to a reference

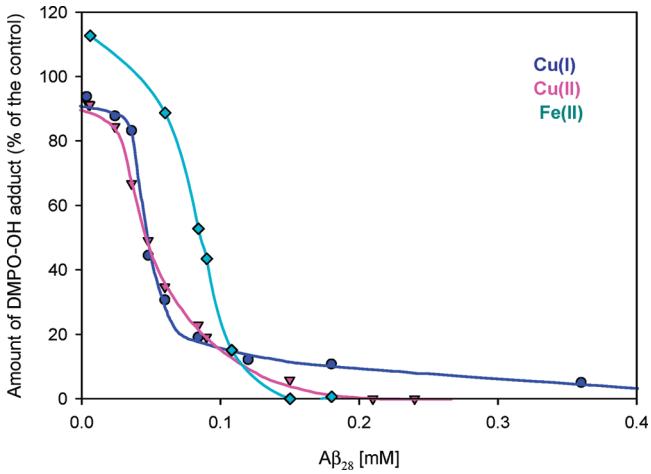

FIGURE 1: Modulation of the Cu(I)/Cu(II)/Fe(II)-induced H_2O_2 decomposition by Aβ_{28} peptide. The reaction was performed in 1 mM Tris buffer, containing 0.1 mM $FeSO_4$ or $Cu(CH_3CN)_4PF_6$ or $Cu(NO_3)_2$, 10 mM H_2O_2, 2 mM DMPO, pH 6.61, 6.62, and 6.60, respectively, and 0−0.36 mM Aβ_{28} peptide. The final Cu(I)−Aβ_{28}−H_2O_2 solution contained 5% v/v acetonitrile. The amount of DMPO−OH adduct is given as the percentage of control, which contains $Cu(CH_3CN)_4PF_6$ or $FeSO_4$ or $Cu(NO_3)_2$, H_2O_2, and DMPO. Curves are an average of 2−5 experiments.

containing Tris buffer, H_2O_2 and Cu(I), and 5% v/v acetonitrile. Likewise, no cupric oxide was obtained at pH 6.60 due to the stabilizing effect of the Tris buffer (*71*). It is noteworthy that, in the presence of metal ion (Fe/Cu) chelators and buffers, the nucleophilic addition of water to DMPO is effectively suppressed (*72*). **(G)** *DMPO Concentration*. The concentration of the spin trap was optimized for the measurement of radical production at both Cu(I)−, Cu(II)−,and Fe(II)−H_2O_2 systems. In Cu(I)-, Cu(II)-, and Fe(II)-induced H_2O_2 decomposition reactions, DMPO was added at a concentration ranging from 1 to 30 mM, and the DMPO−OH adduct peak area was plotted vs DMPO concentration (data not shown). For solutions containing Cu(I), the adduct peak area was linearly dependent on the DMPO concentration up to 15 mM DMPO and then remained almost constant at higher DMPO concentrations. Similarly, in solutions containing Fe(II), the adduct peak area was linearly dependent on a DMPO concentration up to 20 mM DMPO and then remained almost constant at higher DMPO concentrations. For Cu(II)-induced H_2O_2 decomposition, a linear dependence on [DMPO] was also observed, but at ≥25 mM DMPO, degradation of the DMPO−OH adduct was observed. Therefore, for the clear detection of DMPO−OH signals, on the one hand, and the prevention of DMPO−OH degradation, on the other hand, we used 2 mM DMPO for all ESR measurements.

Aβ_{28} Is a Potent Antioxidant. To study the modulatory function of Aβ_{28} at OH radical producing systems, we added 0.1 mM Fe(II), Cu(II), or Cu(I) to Aβ_{28} solutions at the concentration range of 0.6 nM−0.36 mM. Upon the addition of the DMPO spin trap followed by H_2O_2, the concentration of formed OH radicals in these systems (as a percent of control) was evaluated by ESR measurements (Figure 1).

A sigmoidal Aβ concentration-dependent inhibition of OH radical production was observed. Specifically, at 0.6 nM−0.036 mM Aβ no significant reduction was observed, while a decrease of [•OH] was measured at [Aβ] > 0.036 mM. Aβ_{28} inhibited Cu(I)- and Cu(II)-induced H_2O_2 decomposition, respectively, with the same IC_{50} value (0.061 and 0.059 mM for Cu(II) and Cu(I), respectively) (Table 1). This is consistent with a report by Faller et al. published during the submission of our manuscript (*65*).

Table 1: Inhibition of Metal Ion-Induced OH Radical Production by Soluble Aβ_{28} or ADP[a]

	IC_{50} (mM)	
metal ion	Aβ_{28}[b]	ADP
Cu(I)	0.048 ± 0.010 (pH 7.04) 0.059 ± 0.003 (pH 6.62)	0.13 ± 0.03 (*73*)
Cu(II)	0.050 ± 0.004 (pH 6.67) 0.061 ± 0.0005 (pH 6.60)	0.26 ± 0.05 (*73*)
Fe(II)	0.084 ± 0.006 (pH 6.61)	0.14 ± 0.02 (*74*)

[a] IC_{50} values represent the compound's concentration that inhibits 50% of the OH radical production. [b] IC_{50} values were obtained from fitting the Aβ_{28} data to a four-parameter sigmoid curve, with errors being taken as the deviation from the average value.

To evaluate the antioxidant potency of Aβ_{28}, we compared it to potent biological antioxidants we have previously identified (*73, 74*). These antioxidants are Fe/Cu chelators which are based on a nucleotide scaffold. For instance, at the Cu(I)/Cu(II)/Fe(II)−H_2O_2 systems, ADP exhibited the following IC_{50} values: 0.13, 0.26, and 0.14 mM, respectively (Table 1), indicating that Aβ_{28} is a better biological antioxidant.

Chelation vs Scavenging Mechanism. Aβ_{28} can bind specifically 2 equiv of Cu (*53*), and the two Cu(II)-binding sites do not couple. EPR at pH 7.4 showed that Cu is bound in a square-planar geometry and has a mixed coordination of 3N/1O and 4N (the major component is 3N/1O). Asp1 was proposed to coordinate via either the terminal amine or the side-chain carboxylate. The 4N form is dominant at high pH (pH 9), while 3N/1O is dominant at pH 6.5 (*23*). Atwood et al. proposed that there is a very high affinity Cu(II)-binding site on Aβ_{42} (log K_{app} = 17.2) that mediates peptide precipitation. Aβ_{40} has a lower affinity to Cu(II) (ca. log K_{app} 10.3) (*22*). A recent isothermal calorimetry study showed that there are two Cu(II)-binding sites in Aβ_{28} with an apparent K_d of 10^{-7} M^{-1} and 10^{-5} M^{-1}, respectively (*23*). We found that at Aβ:Cu(II) 1:1 ratio there is a 50% reduction of [•OH], whereas at a ca. 2.5:1 ratio there is almost complete inhibition of radical formation (Figure 1). This observation together with the tight Aβ_{28}−Cu binding suggests that inhibition of metal ion-induced H_2O_2 decomposition by Aβ_{28} may be due to metal ion chelation.

In a 2:1 complex, where two Aβ_{28} peptides coordinate with one Cu(II) ion, an octahedral geometry around the Cu(II) ion may be possible via coordination with three His residues (e.g., His6, -13, and -14) of each Aβ unit. In such a geometry, the Cu(II)-coordination sphere is full, and therefore, the coordination of H_2O_2 to Cu(II) (or Fe(II)) and, subsequently, electron transfer reactions are prevented, resulting in inhibition of OH radical formation.

The complete reduction of •OH concentration at the Fe(II)−H_2O_2 system occurs at a 2.5:1 Aβ_{28}:Fe(II) ratio (as for Cu(II)). However, a 50% reduction of [•OH] at the Fe(II)−H_2O_2 system occurs at about a 1.5:1 ratio, as compared to a ca. 1:1 ratio in the Cu−H_2O_2 systems. This difference possibly reflects the lower affinity of Fe(II) to Aβ_{28} as compared to that of Cu(II) (*22, 31, 37*).

Although Aβ_{28} is an efficient metal ion chelator, we cannot exclude a scavenging mechanism where the antioxidant

activity of Aβ could occur due to OH radical scavenging by Aβ's CH moieties.

Indeed, the large numbers of oxidative markers that have been identified in the AD brain indicate that oxygen radical damage may play a role in the etiology of the disease (*20, 75, 76*). Atwood et al. provided further evidence that Cu (but not Fe) coordination promotes histidine modification of Aβ in vivo (*77*). These authors replicated the decrease in the content of histidine residues in vitro by incubating synthetic Aβ with H_2O_2 and Cu(II) (but not Fe(III)). Incubation of $A\beta_{40}$ with Cu(II)−H_2O_2 for 1 day promoted increased loss of His residues (−79%). Since Aβ can reduce Cu(II), producing Cu(I) and H_2O_2 (and consequently •OH), the oxidative modifications were proposed to result from OH radical scavenging by His residues.

Oxidative modification by H_2O_2 of the histidine in the active site of Cu,Zn-SOD resulted in the formation of 2-oxohistidine (*78, 79*). Likewise, Atwood et al. reported that the metal-dependent redox activity leads to carbonylation of Aβ (*22, 77*).

Specifically, OH radicals are formed from H_2O_2 in the vicinity of the redox-active metal ion, which is in turn coordinated by His residues and Asp residues (*23*). Due to the extremely short life of OH radicals, it may be expected that the oxidative damage will be most pronounced in the vicinity of the redox-active metal ion. If indeed the scavenging mechanism is dominant, several oxidation reactions may occur. For instance, the imidazole moiety of His residues may be oxidized to 2-imidazolidinone (*77*), Asp1 may be oxidized to α-oxo acid, and the peptide backbone might undergo cleavages at the metal ion coordination site (*80, 81*).

Specific cleavages of peptide bonds can be mediated by Fe(II) or Cu(II) chelates in the presence of H_2O_2 and ascorbate (*82*). Peptide bonds close to the bound Fe(II)/Cu(II) ion are cleaved by locally generated hydroxyl radicals, via an oxidative cleavage mechanism or via hydrolytic cleavage mechanism (*80, 81*). We found that Cu(II) was a more efficient cleaving reagent as compared to Fe(II) in cleavage of peptide bonds in NTPDase1 (Y. Richter and B. Fischer, unpublished results).

If the dominant antioxidative mechanism is metal ion chelation (i.e., prevention of •OH formation), then we expect the above-mentioned oxidative modifications of $A\beta_{28}$ to be minor. To test this hypothesis, we incubated $A\beta_{28}$ with and without H_2O_2 and Cu(I), Cu(II), or Fe(II) and monitored any changes in the amino acid composition of the peptide−Cu(I)/Fe(II) complex after 4 min (ESR measurement time) or 24 h, and for 21.5 min (ESR measurement time) or 24 h for Cu(II), at pH 7.4. $A\beta_{28}$ samples in Cu/Fe−H_2O_2 were evaluated by an amino acid analyzer as compared to $A\beta_{28}$ samples containing Cu/Fe ions in the absence of H_2O_2. The latter controls are required as Cu/Fe ions create an oxidative environment by inducing the formation of H_2O_2 from atmospheric oxygen.

The quantity of histidine found in each sample is presented as a percentage of the calibration factor. The calibration factor represents 100% amino acid quantity for a given sample. In the sample containing only the peptide, $A\beta_{28}$, the quantity of histidine was 101%; namely, histidine was intact.

Minute degradation of histidine was observed in $A\beta_{28}$ in the presence of metal ions without the addition of H_2O_2. Specifically, upon the addition of Cu(I) or Fe(II) to $A\beta_{28}$ 94.93% and 84.36% His, respectively, remained intact after 4 min incubation. A similar result was obtained for a sample containing $A\beta_{28}$ and Cu(II) where 98% His remained unchanged after 21.5 min incubation.

The addition of H_2O_2 to the samples, under the same conditions, resulted in 74.26% or 81.57% intact His for Cu(I)- or Fe(II)-containing samples, respectively, after a 4 min incubation period. 62.99% His was determined after incubation of $A\beta_{28}$ and Cu(II) with H_2O_2 for 21.5 min. Namely, at ESR measurement conditions, the actual radical production inhibitor, $A\beta_{28}$, acts mainly as a metal ion chelator.

Incubation of $A\beta_{28}$ with Cu(I)/Fe(II)/Cu(II) for 24 h resulted in 89.84%/79.85%/96% His residues, respectively, for the H_2O_2-free sample, consistent with literature (*77*). However, for samples containing H_2O_2 which were incubated for 24 h, only 49.22%/62.74%/23% His remained for Cu(I)/Fe(II)/Cu(II)−H_2O_2, respectively. On prolonged incubation, we observed a more significant His oxidation (due to radical scavenging), as compared to oxidation at ESR conditions. Oxidation of $A\beta_{28}$ in the Cu(I)/Cu(II)−H_2O_2 system was larger than in the Fe(II)−H_2O_2 system. These results may be attributed to the greater affinity of Cu vs Fe to Aβ.

Apparentl, the primary antioxidant activity of Aβ is mainly due to metal ion chelation. This chelation provides a partially full or full coordination sphere, thereby inhibiting electron transfer from the metal ion to H_2O_2 and reducing the amount of OH radicals formed. In addition to the rapid metal chelation mechanism, a secondary scavenging mechanism operates in a time-dependent manner. Small amounts of OH radicals are trapped by Cu(I)/Fe(II)-coordinating His moieties, resulting in the oxidation of these His residues.

For Cu(II), the scavenging mechanism seems to be an important mode of $A\beta_{28}$ antioxidant activity, as compared to Cu(I) and Fe(II). Indeed, we observed a difference in the time-dependent formation of OH radicals in Cu(II)− vs Cu(I)− and Fe(II)−H_2O_2 systems (Figure 3 vs Figure 2).

Modulation of OH Radical Formation by $A\beta_{28}$ Is Time-Dependent. We next studied the time-dependent modulation of •OH production by $A\beta_{28}$ (Figures 2 and 3). At the Cu(I)− and Fe(II)−H_2O_2 systems, where OH radicals are instantaneously produced via Fenton chemistry, we observed only the exponential decay of the DMPO−OH adduct (Figure 2). For instance, at 0.06 mM $A\beta_{28}$ in the Fe(II)−H_2O_2 system, the DMPO−OH adduct concentration completely diminished after 20 min (Figure 2B). The same time-dependent exponential decay of the DMPO−OH adduct concentration was observed for both the control solutions (metal ion/H_2O_2) and solutions containing $A\beta_{28}$ (at 0.024−0.36 mM concentration range). The first measured time point for $A\beta_{28}$−metal ion−H_2O_2 solutions (4 min after H_2O_2 addition) indicated a reduced DMPO−OH adduct concentration, as compared to control, due to metal ion chelation by $A\beta_{28}$. Reduction of the DMPO−OH concentration as a function of time, as compared to control, is due to scavenging mechanisms.

At the Cu(II)−H_2O_2 system, we observed a time-dependent increase in OH radical production (Figure 3). This time-dependent change of the DMPO−OH concentration appeared also in the presence of $A\beta_{28}$, although 0.06 mM $A\beta_{28}$ reduced [•OH] by 50% as compared to control. This finding is consistent with the results of Faller et al. (*65, 83*) Previously, we have attempted the quantification of OH radicals in the

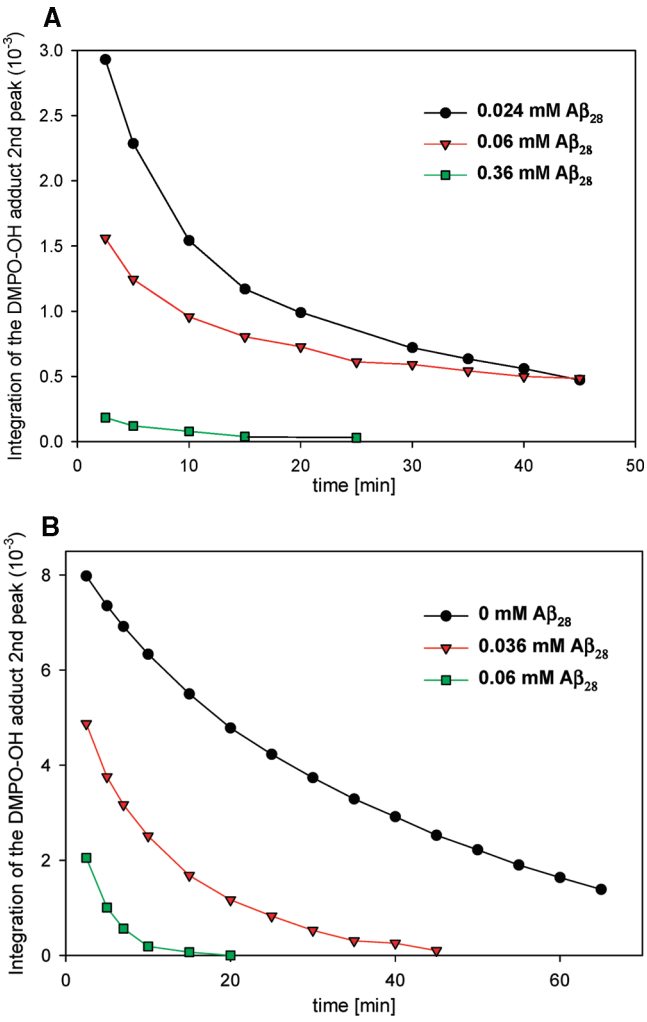

FIGURE 2: Time-dependent curves for the amount of DMPO−OH adduct generated in (A) Cu(I)-induced H_2O_2 decomposition and (B) Fe(II)-induced H_2O_2 decomposition. Reactions were performed by the addition of 10 mM H_2O_2 to solutions containing 0.1 mM $Cu(CH_3CN)_4PF_6$ or $FeSO_4$, 2 mM DMPO, and 1 mM Tris buffer (pH 7.04 for Cu(I) or 6.61 for Fe(II)) in the presence of 0−0.36 mM Aβ_{28}. The zero time point was H_2O_2 addition time as described in Experimental Procedures. The final Cu(I) system solution contained 5% v/v acetonitrile.

Cu(II)−H_2O_2 system (data not shown) and found less than 1 turnover radical production. We have noticed a complex kinetics which is the result of at least two simultaneous kinetic processes: formation of DMPO−OH adduct by the Haber−Weiss-like reaction and decomposition of DMPO−OH adduct.

Modulation of •OH Formation by Aβ_{28} Aggregates. **(A)** *Formation of Aβ_{28}−Cu(I) Aggregates.* A previous report suggested that there is no difference between the binding mode of Cu to either soluble Aβ_{28} or fibrils, as detected by EPR (*84*). This observation may imply that there may not be any difference in the functionality of either soluble or aggregated Aβ_{28}.

To test this hypothesis, we also studied the modulatory function of aggregated Aβ_{28} at oxidative systems.

Aggregation of Aβ_{28} was reported to occur at the physiologically irrelevant 1:10 peptide:Cu(II) molar ratio only after 1 h of incubation (pH 7.3) (*85*).

We attempted to produce 1:1 Aβ_{28}:Cu(I) aggregates at a physiological pH. For this purpose, we produced aggregates

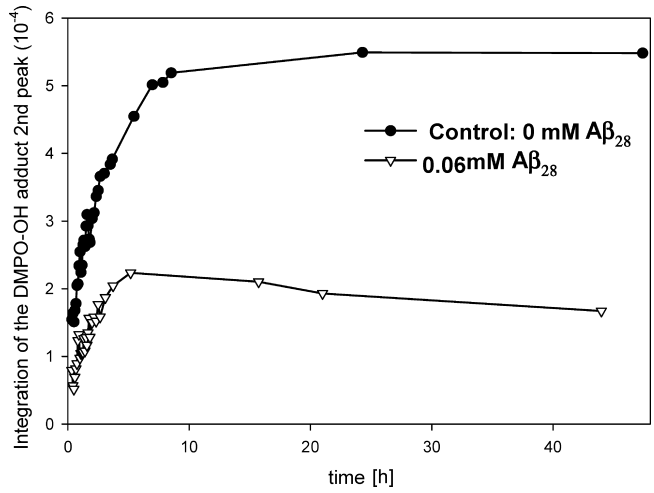

FIGURE 3: Modulation of the Cu(II)-induced H_2O_2 decomposition by Aβ_{28}. The reaction was performed by the addition of 10 mM H_2O_2 to a solution containing 0.1 mM $Cu(NO_3)_2$, 2 mM DMPO, in 1 mM Tris buffer, pH 6.76, and 0.06 mM Aβ_{28}. The amount of DMPO−OH adduct is given as the percentage of control, which contains $Cu(NO_3)_2$, H_2O_2, and DMPO.

of Aβ_{28}:Cu(I) complexes by slowly increasing the pH of this solution from 5 to 7.5, followed by incubation for 30 min at room temperature (see Experimental Procedures).

To characterize the Aβ_{28}−Cu(I) aggregate and to find whether free Cu(I)/Aβ_{28} is available in the ESR sample, we filtered the Aβ_{28}−Cu(I) aggregate from a simulated ESR sample and analyzed the filtrate by ICP measurement.

We found that, in the ESR sample, practically all Cu(I) was coordinated to Aβ_{28}. Only negligible amounts of free Cu(I) (0.007% of starting Cu(I)) were detected. As a control showing that Cu (in the absence of Aβ_{28} aggregates) can quantitatively pass the filter, we incubated overnight $Cu(CH_3CN)_4PF_6$ under the conditions of the above Aβ_{28}:Cu(I) aggregate ICP sample (see Experimental Procedures). ICP data showed that all Cu in the above solution passed through the filter (100% of starting Cu(I) were detected by ICP).

(B) *Characterization of Aβ_{28}:Cu(I) 1:1 Aggregates.* An amyloid fibril is characterized by several criteria including electron microscopy demonstration of fine nonbranching fibers and the presence of a characteristic β-sheet structure.

Aβ_{28}−Cu(I) aggregates were characterized by TEM measurements. TEM images showed rod-like aggregates (length, 182.11 ± 8.57 nM; diameter, 14.56 ± 0.94 nM) (Figure 4A). In most cases, the rods further stacked to form clusters (length, 449.59 ± 38.97 nM; diameter, 73.6 ± 2.32 nM) (Figure 4B). These results are consistent with previously reported data for A$\beta_{40/42}$ protofibrils (*86, 87*).

We confirmed that Aβ_{28}−Cu(I) aggregation was due to β-sheet H-bonding between parallel strands using Congo red and thioflavin-T (ThT) dyes. These dyes stain specifically amyloid fibrils with a β-sheet secondary structure, and the intensity of the dye signal (detected by fluorescence or UV spectroscopy) is enhanced upon binding the β-sheet fibrils (*59–61*). The enhancement of both ThT and Congo red signals in the presence of Aβ_{28}−Cu(I) aggregates proved that the latter has a typical β-sheet fibril structure (Figure 5). A slight shift of the absorption wavelength of Congo red Aβ_{28}−Cu(I) relative to Congo red was observed at 491 vs 487 nm, respectively (not shown). The small shift with

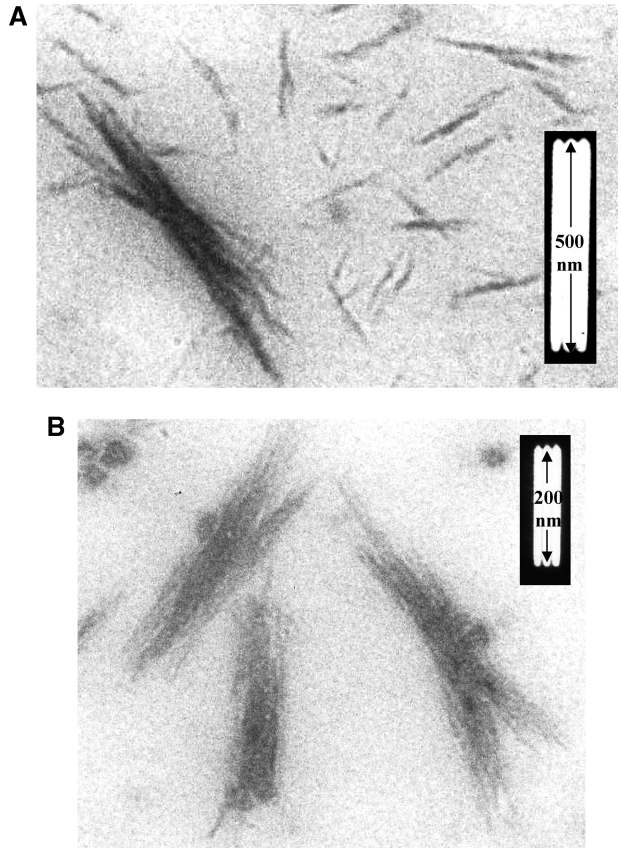

FIGURE 4: TEM images of the Aβ28−Cu(I) aggregates: (A) 200 nm rods; (B) 500 nm bundles. The aggregates were prepared by incubating 0.2 mM $Cu(CH_3CN)_4PF_6$ in acetonitrile and 0.12 mM Aβ28 in water; the solution pH was adjusted to 7.5 by 0.025 M NaOH. The final sample contained 5% v/v acetonitrile.

Congo red is likely due to the fact that Congo red reacts well with mature fibrils but not with premature fibrils.

(C) *Modulation of OH Radical Production by Aggregated Aβ28−Cu(I).* To study the modulatory function of aggregated Aβ28−Cu(I) complex, we added DMPO to the 0.06 mM Aβ28−Cu(I) aggregate suspension in 1 mM Tris buffer, pH 7.4. We then added H_2O_2 and monitored its time-dependent antioxidant activity, as compared to control (0 mM Aβ28) and 0.06 mM soluble Aβ28 (Figure 6).

The aggregated Aβ28−Cu(I) complex reduced OH radical formation as compared to control during the first 10 min, however, far less effectively as compared to soluble Aβ28. As there are practically no free Cu(I) ions in the ESR sample of aggregated Aβ28−Cu(I) (ICP detection mentioned above), we hypothesize that unlike soluble Aβ28, in the aggregated state, Cu(I) ions may have free coordination sites. This may result in higher OH radical production, as compared to soluble Aβ28−Cu(I) complex.

CONCLUSIONS

We found that Aβ28, a soluble Aβ40/42 model, functioned as a potent antioxidant at micromolar concentrations, in cell-free oxidative systems, involving Cu(I)/Fe(II)/Cu(II)-induced OH radical formation.

The formation of Aβ−Cu/Fe aggregates significantly reduces Aβ's antioxidant ability. The smaller inhibition of •OH production in Aβ28−Cu aggregate, as compared to the soluble Aβ28−Cu complex, is probably due to a less efficient

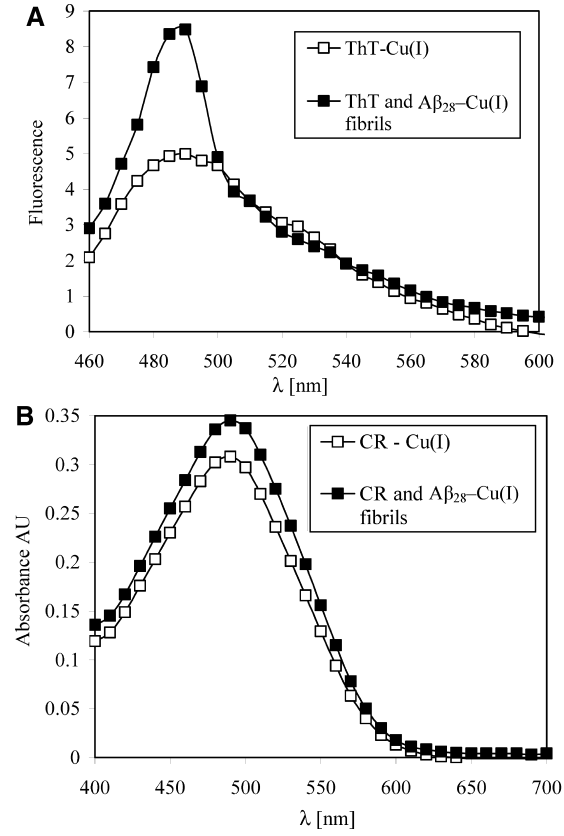

FIGURE 5: Aβ28−Cu(I) fibril dye-binding assays. (A) Emission spectra at 482 nm of 50 μM Thioflavin T and 20 μM $Cu(CH_3CN)_4PF_6$ in PBS (final pH 7.4) in the absence or presence of Aβ28 fibrils. (B) Absorbance spectra of 10 μM Congo red (CR) and 20 μM $Cu(CH_3CN)_4PF_6$ in PBS (pH 7.4) in the absence or presence of Aβ28 fibrils. The fibrils were prepared by incubating 20 μM $Cu(CH_3CN)_4PF_6$ and 12 μM Aβ28; the pH was adjusted to about 7.5 by (0.025 M) NaOH. The final samples in both (A) and (B) contained 5% v/v acetonitrile.

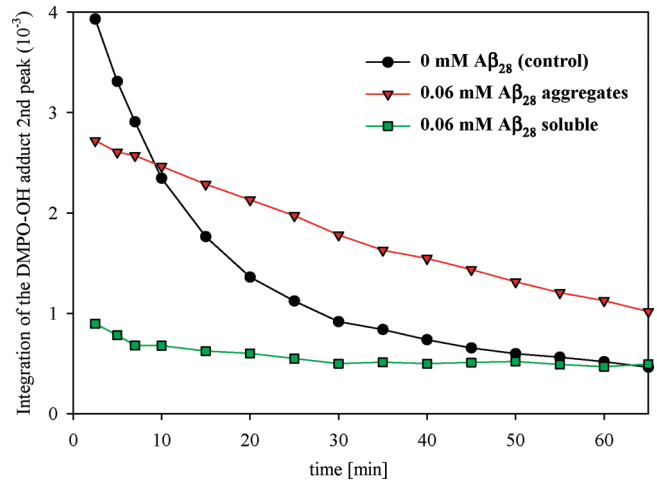

FIGURE 6: Time-dependent curves for the amount of DMPO−OH adduct generated in Cu(I)-induced H_2O_2 decomposition. Reactions were performed in 1 mM Tris buffer, by 0.06 mM $Cu(CH_3CN)_4PF_6$, 10 mM H_2O_2, and 2 mM DMPO, in the presence of 0.06 mM soluble (pH 7.04) or aggregated Aβ28 (pH 7.5). The final samples contained 5% v/v acetonitrile. The zero time point was H_2O_2 addition as described in Experimental Procedures.

metal ion chelation and scavenging mechanisms in Aβ28−Cu aggregate. Less efficient chelation is possibly related to the β-sheet arrangement of Aβ in aggregates. The β-sheet arrangement does not allow for regular Cu chelation by all

three His residues (His6, -13, -14) and therefore allows an electron transfer from Cu to H_2O_2 to occur more efficiently. This efficient transfer results in higher •OH production, compared to soluble Aβ_{28}−Cu(Fe) complex.

The mode of antioxidant activity of soluble Aβ_{28} is twofold. The primary (rapid) mechanism involves metal chelation and inhibition of electron transfer from Cu/Fe to H_2O_2. The secondary (slow) mechanism involves OH radical scavenging and oxidation of Cu(Fe)-coordinating ligands (His residues). Namely, Aβ_{28} functions as an antioxidant, yet it is partially oxidized itself. This phenomenon is especially severe in the presence of Cu(II). However, as under physiological conditions Cu(II) is reduced to Cu(I) (by A$\beta_{40/42}$ Met35 or cellular reductants), the oxidation of Aβ_{28} (and possibly A$\beta_{40/42}$) by Cu(I)−H_2O_2 is much slower.

Possible Physiological Implications of Our Findings. The modulation of oxidative conditions (e.g., H_2O_2−Cu) by A$\beta_{40/42}$ presumably occurs primarily in Aβ's metal ion coordinating region (His6, His13, His14), included in Aβ_{28}. Yet, A$\beta_{40/42}$'s Met35, proposed to play a role in the modulation of cellular oxidation by reducing Cu(II) to Cu(I), is lacking in Aβ_{28}. To overcome the absence of Met35 in Aβ_{28} and cellular reductants, we directly studied the Aβ_{28}−Cu(I) complex. In this way we believe we have mimicked A$\beta_{40/42}$ modulation of oxidative conditions.

It is assumed that endogenous A$\beta_{40/42}$ reduces molecular oxygen to •OH ($O_2 \rightarrow O_2^{-\bullet} \rightarrow H_2O_2 \rightarrow$ •OH) (*37*). In the present study, we have focused on only part of the reduction pathway, namely, the reduction of H_2O_2 to •OH. Yet, as •OH is the most deleterious ROS, and as we closely mimicked A$\beta_{40/42}$−metal ion complexes by Aβ_{28}−Cu(I)/Fe(II) complexes, we believe we can point to several implications of our findings to physiological systems.

In a healthy brain, Cu and Aβ's concentrations are estimated as 70 μM (*21, 22*) and low nanomolar concentration range (*43, 88*), respectively. At these Cu and Aβ concentrations, we do not expect any protective effect of Aβ based on our findings showing no inhibition of H_2O_2 decomposition induced by 100 μM Cu(I)/(II), at nanomolar Aβ concentrations. Yet, in an AD brain Cu (ca. 400 μM *21, 22*) and Aβ's (*43*) concentrations are significantly elevated. Earlier reports described neurotoxic activity of Aβ at micromolar concentration (*51, 52*). As soluble Aβ_{28} inhibited •OH production with IC_{50} of 59 and 84 μM, at 100 μM Cu(I) and Fe(II), we believe that Aβ may play a protective role in the early stages of AD, but not in healthy individuals, where Aβ's concentrations are nanomolar. Yet, as Aβ−metal ion complexes undergo aggregation, they significantly lose their protective function and allow oxidative damage to occur.

We believe that the data presented here provide a solution to the long-standing dispute on Aβ's role in health and disease.

Our results prompted us to study the effect of Aβ_{40} on the modulation of Cu/Fe-induced H_2O_2 decomposition in a cell-free system, under the experimental conditions described above. These results will be published in due course.

ACKNOWLEDGMENT

The authors express their graditude to Dr. Arye Tishbee, Department of Chemistry, Weizmann Institute, Israel, for performing amino acid analysis.

REFERENCES

1. Case, F. (2005) Metal for the mind. *Chem. World 2*, 28–32.
2. Qureshi, G. A., Memon, S. A., Memon, A. B., Ghouri, R. A., Memon, J. M., and Parvez, S. H. (2005) The emerging role of iron, zinc, copper, magnesium and selenium and oxidative stress in health and diseases. *Biog. Amines 19*, 147–169.
3. Uriu-Adams, J. Y., and Keen, C. L. (2005) Copper, oxidative stress, and human health. *Mol. Aspects Med. 26*, 268–298.
4. Korycka, D., Malgorzata, B., and Richardson, T. (1978) Activated oxygen species and oxidation of food constituents. *Crit. Rev. Food Sci. Nutr. 10*, 209–241.
5. Halliwell, B. (1997) Antioxidants and human disease: a general introduction. *Nutr. Rev. 55*, S44–S49; discussion S49−S52.
6. Fenton, H. J. H. (1894) *J. Chem. Soc. 65*, 899.
7. Halliwell, B., Gutteridge, J. M. C., and Aruoma, O. I. (1987) The deoxyribose method: a simple "test-tube" assay for determination of rate constants for reactions of hydroxyl radicals. *Anal. Biochem. 165*, 215–219.
8. Burkitt, M. J., Tsang, S. Y., Tam, S. C., and Bremner, I. (1995) Generation of 5,5-dimethyl-1-pyrroline N-oxide hydroxyl and scavenger radical adducts from copper/H_2O_2 mixtures: effects of metal ion chelation and the search for high-valent metal-oxygen intermediates. *Arch. Biochem. Biophys. 323*, 63–70.
9. Haber, F., and Weiss, J. (1934) The catalytic decomposition of hydrogen peroxide by iron salts. *Proc. R. Soc. London A147*, 332–351.
10. Weiss, J. (1935) Electron transition processes in the mechanism of oxidation and reduction reactions in solutions. *Naturwissenschaften 23*, 64–69.
11. Barb, W. G., Baxendale, J. H., George, P., and Hargrave, K. R. (1951) Reactions of ferrous and ferric ions with hydrogen peroxide. I. Ferrous-ion reaction. *Trans. Faraday Soc. 47*, 462–500.
12. Pecci, L., Montefoschi, G., and Cavallini, D. (1997) Some new details of the copper-hydrogen peroxide interaction. *Biochem. Biophys. Res. Commun. 235*, 264–267.
13. Gutteridge, J. M. C., and Wilkins, S. (1983) Copper salt-dependent hydroxyl radical formation. Damage to proteins acting as antioxidants. *Biochim. Biophys. Acta 759*, 38–41.
14. Behl, C., Davis, J. B., Lesley, R., and Schubert, D. (1994) Hydrogen peroxide mediates amyloid β protein toxicity. *Cell 77*, 817–827.
15. Tomiyama, T., Shoji, A., Kataoka, K.-i., Suwa, Y., Asano, S., Kaneko, H., and Endo, N. (1996) Inhibition of amyloid β protein aggregation and neurotoxicity by rifampicin. Its possible function as a hydroxyl radical scavenger. *J. Biol. Chem. 271*, 6839–6844.
16. Huang, X., Moir, R. D., Tanzi, R. E., Bush, A. I., and Rogers, J. T. (2004) Redox-active metals, oxidative stress, and Alzheimer's disease pathology. *Ann. N.Y. Acad. Sci. 1012*, 153–163.
17. Glenner, G. G., and Wong, C. W. (1984) Alzheimer's disease: initial report of the purification and characterization of a novel cerebrovascular amyloid protein. *Biochem. Biophys. Res. Commun. 120*, 885–890.
18. Masters, C. L., Simms, G., Weinman, N. A., Multhaup, G., McDonald, B. L., and Beyreuther, K. (1985) Amyloid plaque core protein in Alzheimer disease and Down syndrome. *Proc. Natl. Acad. Sci. U.S.A. 82*, 4245–4249.
19. Selkoe, D. J. (1991) The molecular pathology of Alzheimer's disease. *Neuron 6*, 487–498.
20. Atwood, C. S., Huang, X., Moir, R. D., Tanzi, R. E., and Bush, A. I. (1999) Role of free radicals and metal ions in the pathogenesis of Alzheimer's disease. *Metal Ions Biol. Sys. 36*, 309–364.
21. Lovell, M. A., Robertson, J. D., Teesdale, W. J., Campbell, J. L., and Markesbery, W. R. (1998) Copper, iron and zinc in Alzheimer's disease senile plaques. *J. Neurol. Sci. 158*, 47–52.
22. Atwood, C. S., Scarpa, R. C., Huang, X., Moir, R. D., Jones, W. D., Fairlie, D. P., Tanzi, R. E., and Bush, A. I. (2000) Characterization of copper interactions with Alzheimer amyloid β peptides: identification of an attomolar-affinity copper binding site on amyloid β1−42. *J. Neurochem. 75*, 1219–1233.
23. Guilloreau, L., Damian, L., Coppel, Y., Mazarguil, H., Winterhalter, M., and Faller, P. (2006) Structural and thermodynamical properties of CuII amyloid-β16/28 complexes associated with Alzheimer's disease. *J. Biol. Inorg. Chem. 11*, 1024–1038.
24. Dong, J., Atwood, C. S., Anderson, V. E., Siedlak, S. L., Smith, M. A., Perry, G., and Carey, P. R. (2003) Metal binding and oxidation of amyloid-β within isolated senile plaque cores: Raman microscopic evidence. *Biochemistry 42*, 2768–2773.
25. Atwood, C. S., Moir, R. D., Huang, X., Scarpa, R. C., Bacarra, N. M. E., Romano, D. M., Hartshorn, M. A., Tanzi, R. E., and

Bush, A. I. (1998) Dramatic aggregation of Alzheimer Aβ by Cu(II) is induced by conditions representing physiological acidosis. *J. Biol. Chem. 273*, 12817–12826.
26. Curtain, C. C., Ali, F., Volitakis, I., Cherny, R. A., Norton, R. S., Beyreuther, K., Barrow, C. J., Masters, C. L., Bush, A. I., and Barnham, K. J. (2001) Alzheimer's disease amyloid-β binds copper and zinc to generate an allosterically ordered membrane-penetrating structure containing superoxide dismutase-like subunits. *J. Biol. Chem. 276*, 20466–20473.
27. Malouf, A. T. (1992) Effect of beta amyloid peptides on neurons in hippocampal slice cultures. *Neurobiol. Aging 13*, 543–551.
28. Pike, C. J., Walencewicz, A. J., Glabe, C. G., and Cotman, C. W. (1991) Aggregation-related toxicity of synthetic β-amyloid protein in hippocampal cultures. *Eur. J. Pharmacol. 207*, 367–368.
29. Pike, C. J., Burdick, D., Walencewicz, A. J., Glabe, C. G., and Cotman, C. W. (1993) Neurodegeneration induced by β-amyloid peptides in vitro: the role of peptide assembly state. *J. Neurosci. 13*, 1676–1687.
30. Lambert, M. P., Barlow, A. K., Chromy, B. A., Edwards, C., Freed, R., Liosatos, M., Morgan, T. E., Rozovsky, I., Trommer, B., Viola, K. L., Wals, P., Zhang, C., Finch, C. E., Krafft, G. A., and Klein, W. L. (1998) Diffusible, nonfibrillar ligands derived from Abeta1−42 are potent central nervous system neurotoxins. *Proc. Natl. Acad. Sci. U.S.A. 95*, 6448–6453.
31. Huang, X., Cuajungco, M. P., Atwood, C. S., Hartshorn, M. A., Tyndall, J. D. A., Hanson, G. R., Stokes, K. C., Leopold, M., Multhaup, G., Goldstein, L. E., Scarpa, R. C., Saunders, A. J., Lim, J., Moir, R. D., Glahe, C., Bowden, E. F., Masters, C. L., Fairlie, D. P., Tanzi, R. E., and Bush, A. I. (1999) Cu(II) potentiation of Alzheimer Aβ neurotoxicity. Correlation with cell-free hydrogen peroxide production and metal reduction. *J. Biol. Chem. 274*, 37111–37116.
32. Whitson, J. S., Glabe, C. G., Shintani, E., Abcar, A., and Cotman, C. W. (1990) β-Amyloid protein promotes neuritic branching in hippocampal cultures. *Neurosci. Lett. 110*, 319–324.
33. Rottkamp, C. A., Raina, A. K., Zhu, X., Gaier, E., Bush, A. I., Atwood, C. S., Chevion, M., Perry, G., and Smith, M. A. (2001) Redox-active iron mediates amyloid-β toxicity. *Free Radical Biol. Med. 30*, 447–450.
34. Schubert, D., and Chevion, M. (1995) The role of iron in beta amyloid toxicity. *Biochem. Biophys. Res. Commun. 216*, 702–707.
35. Barrow, C. J., Yasuda, A., Kenny, P. T. M., and Zagorski, M. G. (1992) Solution conformations and aggregational properties of synthetic amyloid β-peptides of Alzheimer's disease. Analysis of circular dichroism spectra. *J. Mol. Biol. 225*, 1075–1093.
36. Zagorski, M. G., and Barrow, C. J. (1992) NMR studies of amyloid β-peptides: proton assignments, secondary structure, and mechanism of an α-helix → β-sheet conversion for a homologous, 28-residue, N-terminal fragment. *Biochemistry 31*, 5621–5631.
37. Huang, X., Atwood, C. S., Hartshorn, M. A., Multhaup, G., Goldstein, L. E., Scarpa, R. C., Cuajungco, M. P., Gray, D. N., Lim, J., Moir, R. D., Tanzi, R. E., and Bush, A. I. (1999) The Aβ peptide of Alzheimer's disease directly produces hydrogen peroxide through metal ion reduction. *Biochemistry 38*, 7609–7616.
38. Bush, A. I., Masters, C. L., and Tanzi, R. E. (2003) Copper, β-amyloid, and Alzheimer's disease: Tapping a sensitive connection. *Proc. Natl. Acad. Sci. U.S.A. 100*, 11193–11194.
39. Irie, K., Murakami, K., Masuda, Y., Morimoto, A., Ohigashi, H., Ohashi, R., Takegoshi, K., Nagao, M., Shimizu, T., and Shirasawa, T. (2005) Structure of β-amyloid fibrils and its relevance to their neurotoxicity: Implications for the pathogenesis of Alzheimer's disease. *J. Biosci. Bioeng. 99*, 437–447.
40. Smith, M. A., Nunomura, A., Zhu, X., Takeda, A., and Perry, G. (2000) Metabolic, metallic, and mitotic sources of oxidative stress in Alzheimer disease. *Antiox. Redox Signal. 2*, 413–420.
41. Smith, M. A., Joseph, J. A., and Perry, G. (2000) Arson. Tracking the culprit in Alzheimer's disease. *Ann. N.Y. Acad. Sci. 924*, 35–38.
42. Shigenaga, M. K., Hagen, T. M., and Ames, B. N. (1994) Oxidative damage and mitochondrial decay in aging. *Proc. Natl. Acad. Sci. U.S.A. 91*, 10771–10778.
43. Atwood, C. S., Obrenovich, M. E., Liu, T., Chan, H., Perry, G., Smith, M. A., and Martins, R. N. (2003) Amyloid-β: a chameleon walking in two worlds: a review of the trophic and toxic properties of amyloid-β. *Brain Res. Rev. 43*, 1–16.
44. Behl, C., Davis, J., Cole, G. M., and Schubert, D. (1992) Vitamin E protects nerve cells from amyloid β protein toxicity. *Biochem. Biophys. Res. Commun. 186*, 944–950.
45. Kontush, A., Berndt, C., Weber, W., Akopyan, V., Arlt, S., Schippling, S., and Beisiegel, U. (2001) Amyloid-β is an antioxidant for lipoproteins in cerebrospinal fluid and plasma. *Free Radical Biol. Med. 30*, 119–128.
46. Zou, K., Gong, J.-S., Yanagisawa, K., and Michikawa, M. (2002) A novel function of monomeric amyloid β-protein serving as an antioxidant molecule against metal-induced oxidative damage. *J. Neurosci. 22*, 4833–4841.
47. Andorn, A. C., and Kalaria, R. N. (2000) Factors affecting pro- and anti-oxidant properties of fragments of the β-protein precursor (bPP): Implication for Alzheimer's disease. *J. Alzheimer's Dis. 2*, 69–78.
48. Gibson, G. E., Zhang, H., Sheu, K. F. R., and Park, L. C. H. (2000) Differential alterations in antioxidant capacity in cells from Alzheimer patients. *Biochim. Biophys. Acta, Mol. Basis Dis. 1502*, 319–329.
49. Kontush, A., Donarski, N., and Beisiegel, U. (2001) Resistance of human cerebrospinal fluid to in vitro oxidation is directly related to its amyloid-β content. *Free Radical Res. 35*, 507–517.
50. Bush, A. I. (2000) Metals and neuroscience. *Curr. Opin. Chem. Biol. 4*, 184–191.
51. Varadarajan, S., Yatin, S., Aksenova, M., and Butterfield, D. A. (2000) Review: Alzheimer's amyloid β-peptide-associated free radical oxidative stress and neurotoxicity. *J. Struct. Biol. 130*, 184–208.
52. Markesbery, W. R. (1997) Oxidative stress hypothesis in Alzheimer's disease. *Free Radical Biol. Med. 23*, 134–147.
53. Syme, C. D., Nadal, R. C., Rigby, S. E. J., and Viles, J. H. (2004) Copper binding to the amyloid-β (Aβ) peptide associated with Alzheimer's disease: Folding, coordination geometry, pH dependence, stoichiometry, and affinity of Aβ-(1−28): Insights from a range of complementary spectroscopic techniques. *J. Biol. Chem. 279*, 18169–18177.
54. Talafous, J., Marcinowski, K. J., Klopman, G., and Zagorski, M. G. (1994) Solution structure of residues 1−28 of the amyloid β-peptide. *Biochemistry 33*, 7788–7796.
55. Shen, C. L., Scott, G. L., Merchant, F., and Murphy, R. M. (1993) Light scattering analysis of fibril growth from the amino-terminal β(1−28) of β-amyloid peptide. *Biophys. J. 65*, 2383–2395.
56. Brenner, A. J., and Harris, E. D. (1995) A quantitative test for copper using bicinchoninic acid. *Anal. Biochem. 226*, 80–84.
57. Kalyanaraman, B. (1982) Detection of toxic free radicals in biology and medicine. *Rev. Biochem. Toxicol. 4*, 73–139.
58. Gill, S. C., and von Hippel, P. H. (1989) Calculation of protein extinction coefficients from amino acid sequence data. *Anal. Biochem. 182*, 319–326.
59. Mira, H., Vilar, M., Esteve, V., Martinell, M., Kogan Marcelo, J., Giralt, E., Salom, D., Mingarro, I., Penarrubia, L., and Perez-Paya, E. (2004) Ionic self-complementarity induces amyloid-like fibril formation in an isolated domain of a plant copper metallochaperone protein. *BMC Struct. Biol. 4*, 7.
60. Zou, J., Kajita, K., and Sugimoto, N. (2001) Cu^{2+} inhibits the aggregation of amyloid β-peptide (1−42) in vitro. *Angew. Chem., Int. Ed. 40*, 2274–2277.
61. Klunk, W. E., Pettegrew, J. W., and Abraham, D. J. (1989) Quantitative evaluation of Congo red binding to amyloid-like proteins with a beta-pleated sheet conformation. *J. Histochem. Cytochem. 37*, 1273–1281.
62. Ali, F. E., Separovic, F., Barrow, C. J., Yao, S., and Barnham, K. J. (2006) Copper and zinc mediated oligomerization of Aβ peptides. *Int. J. Pept. Res. Therapeut. 12*, 153–164.
63. Jiang, D., Men, L., Wang, J., Zhang, Y., Chickenyen, S., Wang, Y., and Zhou, F. (2007) Redox reactions of copper complexes formed with different β-amyloid peptides and their neuropathalogical relevance. *Biochemistry 46*, 9270–9282.
64. Ciccotosto, G. D., Barnham, K. J., Cherny, R. A., Masters, C. L., Bush, A. I., Curtain, C. C., Cappai, R., and Tew, D. (2004) Methionine oxidation: Implications for the mechanism of toxicity of the β-amyloid peptide from Alzheimer's disease. *Lett. Pept. Sci. 10*, 413–417.
65. Guilloreau, L., Combalbert, S., Sournia-Saquet, A., Mazarguil, H., and Faller, P. (2007) Redox chemistry of copper-amyloid-b: the generation of hydroxyl radical in the presence of ascorbate is linked to redox-potentials and aggregation state. *ChemBioChem 8*, 1317–1325.
66. Hou, L., and Zagorski, M. G. (2006) NMR reveals anomalous copper(II) binding to the amyloid Aβ peptide of Alzheimer's disease. *J. Am. Chem. Soc. 128*, 9260–9261.

67. Ueda, J.-i., Saito, N., and Ozawa, T. (1996) Detection of free radicals produced from reactions of lipid hydroperoxide model compounds with Cu(II) complexes by ESR spectroscopy. *Arch. Biochem. Biophys. 325*, 65–76.
68. Kim, Y. S., and Han, S. (2000) Nitric oxide protects Cu,Zn-superoxide dismutase from hydrogen peroxide-induced inactivation. *FEBS Lett. 479*, 25–28.
69. Rae, T. D., Schmidt, P. J., Pufahl, R. A., Culotta, V. C., and O'Halloran, T. V. (1999) Undetectable intracellular free copper: the requirement of a copper chaperone for superoxide dismutase. *Science 284*, 805–808.
70. Hicks, M., and Gebicki, J. M. (1986) Rate constants for reaction of hydroxyl radicals with Tris, Tricine and Hepes buffers. *FEBS Lett. 199*, 92–94.
71. Gelvan, D., and Saltman, P. (1990) Different cellular targets for copper- and iron-catalyzed oxidation observed using a copper-compatible thiobarbituric acid assay. *Biochim. Biophys. Acta, Gen. Subj. 1035*, 353–360.
72. Hanna, P. M., Chamulitrat, W., and Mason, R. P. (1992) When are metal ion-dependent hydroxyl and alkoxyl radical adducts of 5,5-dimethyl-1-pyrroline N-oxide artifacts? *Arch. Biochem. Biophys. 296*, 640–644.
73. Baruch, R., and Fischer, B. (2007) Can nucleotides prevent Cu-induced oxidative damage?, *J. Inorg. Biochem.* (in press).
74. Richter, Y., and Fischer, B. (2006) Nucleotides and inorganic phosphates as potential antioxidants. *J. Biol. Inorg. Chem. 11*, 1063–1074.
75. Lovell, M. A., Gabbita, S. P., and Markesbery, W. R. (1999) Increased DNA oxidation and decreased levels of repair products in Alzheimer's disease ventricular CSF. *J. Neurochem. 72*, 771–776.
76. Wang, J., Markesbery, W. R., and Lovell, M. A. (2006) Increased oxidative damage in nuclear and mitochondrial DNA in mild cognitive impairment. *J. Neurochem. 96*, 825–832.
77. Atwood, C. S., Huang, X., Khatri, A., Scarpa, R. C., Kim, Y.-S., Moir, R. D., Tanzi, R. E., Roher, A. E., and Bush, A. I. (2000) Copper catalyzed oxidation of Alzheimer Aβ. *Cell. Mol. Biol. 46*, 777–783.
78. Zhao, F., Ghezzo-Schoneich, E., Aced, G. I., Hong, J., Milby, T., and Schoneich, C. (1997) Metal-catalyzed oxidation of histidine in human growth hormone. Mechanism, isotope effects, and inhibition by a mild denaturing alcohol. *J. Biol. Chem. 272*, 9019–9029.
79. Uchida, K., and Kawakishi, S. (1994) Identification of oxidized histidine generated at the active site of Cu,Zn-superoxide dismutase exposed to H2O2. Selective generation of 2-oxo-histidine at the histidine 118. *J. Biol. Chem. 269*, 2405–2410.
80. Berlett, B. S., and Stadtman, E. R. (1997) Protein oxidation in aging, disease, and oxidative stress. *J. Biol. Chem. 272*, 20313–20316.
81. Platis, I. E., Ermacora, M. R., and Fox, R. O. (1993) Oxidative polypeptide cleavage mediated by EDTA-iron covalently linked to cysteine residues. *Biochemistry 32*, 12761–12767.
82. Patchornik, G., Goldshleger, R., and Karlish, S. J. D. (2000) The complex ATP-Fe^{2+} serves as a specific affinity cleavage reagent in ATP-Mg^{2+} sites of Na,K-ATPase: Altered ligation of Fe^{2+} (Mg^{2+}) ions accompanies the E1P$\rightarrow$E2P conformational change. *Proc. Natl. Acad. Sci. U.S.A. 97*, 11954–11959.
83. Murray, I. V. J., Sindoni, M. E., and Axelsen, P. H. (2005) Promotion of oxidative lipid membrane damage by amyloid β proteins. *Biochemistry 44*, 12606–12613.
84. Karr, J. W., Kaupp, L. J., and Szalai, V. A. (2004) Amyloid-β binds Cu^{2+} in a mononuclear metal ion binding site. *J. Am. Chem. Soc. 126*, 13534–13538.
85. Beking, K., Hao, X., Basak, S., and Basak, A. (2005) Modulatory effects of pH, Cu^{+2} and sheet breakers on aggregation of amyloid peptides. *Protein Pept. Lett. 12*, 197–202.
86. Gorman, P. M., and Chakrabartty, A. (2001) Alzheimer β-amyloid peptides: structures of amyloid fibrils and alternate aggregation products. *Biopolymers 60*, 381–394.
87. Walsh, D. M., Hartley, D. M., Kusumoto, Y., Fezoui, Y., Condron, M. M., Lomakin, A., Benedek, G. B., Selkoe, D. J., and Teplow, D. B. (1999) Amyloid β-protein fibrillogenesis. Structure and biological activity of protofibrillar intermediates. *J. Biol. Chem. 274*, 25945–25952.
88. Kuo, Y.-M., Emmerling, M. R., Vigo-Pelfrey, C., Kasumic, T. C., Kirkpatrick, J. B., Murdoch, G. H., Ball, M. J., and Roher, A. E. (1996) Water-soluble Aβ (N-40, N-42) oligomers in normal and Alzheimer disease brains. *J. Biol. Chem. 271*, 4077–4081.

BI800114G